Experimental Neurology 312 (2019) 51–62

Contents lists available at ScienceDirect

Experimental Neurology

journal homepage: www.elsevier.com/locate/yexnr

Research paper

Validation study of neurotrophin-3-releasing chitosan facilitation of neural tissue generation in the severely injured adult rat spinal cord

Martin Oudega[a,b,c,*], Peng Hao[d], Junkui Shang[d], Agnes E. Haggerty[a], Zijue Wang[d,e], Jian Sun[d], Daniel J. Liebl[a,b], Yan Shi[a], Liming Cheng[f,g,h], Hongmei Duan[d], Yi Eve Sun[h,i], Xiaoguang Li[d,e], Vance P. Lemmon[a,b]

[a] The Miami Project to Cure Paralysis, University of Miami Miller School of Medicine, 1095 NW 14th Terrace, Miami, FL 33136-1060, United States
[b] Department of Neurological Surgery, University of Miami Miller School of Medicine, Miami, FL 33136, United States
[c] Bruce W. Carter Department of Veterans Affairs Medical Center, Miami, FL 33136, United States
[d] Department of Neurobiology, School of Basic Medical Sciences, Capital Medical University, Beijing 100069, China
[e] Beijing International Cooperation Bases for Science and Technology on Biomaterials and Neural Regeneration, Beijing Key Laboratory for Biomaterials and Neural Regeneration, Beijing Advanced Innovation Center for Big Data-Based Precision Medicine, Beijing Advanced Innovation Center for Biomedical Engineering, School of Biological Science and Medical Engineering, Beihang University, Beijing 100083, China
[f] Division of Spine Surgery, Department of Orthopedics, Tongji Hospital, Tongji University School of Medicine, Shanghai 200065, China
[g] Institute of Spine and Spine Cord Injury of Tongji University, Shanghai 200065, China
[h] Translational Stem Cell Research Center, Tongji Hospital, Tongji University School of Medicine, Shanghai 200065, China
[i] Department of Psychiatry and Biobehavioral Sciences, UCLA Medical School, Los Angeles, CA 90095, United States

ARTICLE INFO

Keywords:
Spinal cord injury
NT-3
Biomaterial
Regeneration
Neurogenesis
Replication

ABSTRACT

It was previously reported that a tube holding chitosan carriers loaded with neurotrophin-3 (NT-3), after insertion into a 5 mm long transection gap in the adult rat spinal cord, triggered de novo neural tissue generation and functional recovery. Here, we report an effort to validate these findings using stringent blinding methodologies, which are crucial for robustness in reproducing biomedical studies. Radio frequency identification (RFID) chips were utilized to label rats that were randomly assigned into three experimental groups: transection with chitosan-NT-3 implant (C-NT3), transection only (T-controls), and laminectomy only (S-controls), blinding the experimenters to the treatments. Three months after surgery, animals only known by their RFID were functionally, electrophysiologically, and anatomically assessed. The data were then collected into the proper groups and statistically analyzed. Neural tissue with nestin-, Tuj1-, and NeuN-positive cells was found bridging the transection gap in C-NT3 rats, but not in T-controls. Motor- and somatosensory-evoked potentials were detected in C-NT3 rats and S-controls, but not in T-controls. Hind limb movement was significantly better in C-NT3 rats compared with T-controls. Our validation study indicates that C-NT3 implants facilitate neural tissue generation, at least in part, by eliciting endogenous neurogenesis. Our data support the use of C-NT3 implants for tissue remodeling in the injured spinal cord.

1. Introduction

Spinal cord injury (SCI) causes immediate and progressive loss of nervous tissue associated with impaired function (Hagg and Oudega, 2006). Engendering tissue modeling may provide a scaffold for anatomical repair (Chen, 2014). A potentially effective approach to form new tissue in the damaged spinal cord is to harness neurogenesis from the endogenous pool of neural progenitor cells (NPCs; Gage, 2000; Luo et al., 2015). The spinal cord contains NPCs (Alonso, 1999) and their number increases after injury (Yamamoto et al., 2001; Barnabé-Heider et al., 2010). NPCs may migrate and differentiate into neural cells (Barnabé-Heider et al., 2010), a process which is governed by the local microenvironment (Luo et al., 2015). Neurotrophin-3 (NT-3) is important in NPC recruitment and differentiation into neurons (Li et al., 2009a,b; Yang et al., 2010).

Yang et al. (2015) showed the presence of newly generated neural tissue in a tubular chitosan scaffold filled with NT-3-releasing chitosan carriers (i.e., C-NT3 implant) after implantation into the complete

* Corresponding author at: The Miami Project to Cure Paralysis, University of Miami Miller School of Medicine, 1095 NW 14th Terrace, Miami, FL 33136-1060, United States.
E-mail address: moudega@miami.edu (M. Oudega).

https://doi.org/10.1016/j.expneurol.2018.11.003
Received 3 October 2018; Received in revised form 1 November 2018; Accepted 8 November 2018
Available online 22 November 2018

transected adult rat spinal cord. With this particular repair strategy, overground walking gradually improved during the 52 week survival period (Yang et al., 2015). It was concluded that the NT-3-releasing chitosan implant may have significant clinical potential for repairing the spinal cord in people with severe SCI.

The general consensus is that basic and translational biomedical research suffers from a lack in robustness with low success rates in replication studies reported in different scientific areas (Prinz et al., 2011; Begley and Ellis, 2012), including SCI and repair (Steward et al., 2012). Several factors may contribute to this critical problem (Landis et al., 2012), including deficiency in blinding of investigators to treatments (Button et al., 2013; Lazic and Essioux, 2013; Weller, 2018). Preferably, before new promising treatments are tested clinically, the original animal study should be replicated in a stringently blinded study (Kwon et al., 2013). Many factors make such studies difficult or even impossible to complete (Landis et al., 2012; Steward et al., 2012; Callahan et al., 2017). Funding agencies rarely fund replication studies. Institutions are concerned about protecting intellectual property and can restrict transfer of reagents, devices, and even procedures and data. The investigators who do the replication study may encounter difficulty publishing and often get little credit for their work. Finally, research at different institutions and especially in countries with different regulatory environments can prevent strict replications.

The authors of the present work were motivated to validate the findings described in Yang et al. (2015) using an international team of SCI researchers to investigate tissue formation, neurogenesis, electrophysiology, and hind limb function at 3 months after acute implantation of a C-NT3 implant in the complete transected spinal cord of adult rats employing a rigorous blinding strategy. Our findings suggest that the chitosan-based NT-3-releasing implant elicits endogenous neurogenesis and support its potential for tissue modeling in the injured adult spinal cord.

2. Material and methods

2.1. Animals

This study used adult female Wistar rats (SPF, 250–300 g; $n = 19$). Only female rats were used to reproduce the experimental conditions in Yang et al. (2015), which we aimed to validate in the present study. Personnel at the Capital Medical University of Beijing performed all animal-related procedures, acquired blindly all data, and maintained all data records and storage. Investigators from the Miami Project to Cure Paralysis randomized the animals, thereby blinding the surgeons and other investigators to the treatments, and observed all surgeries. Animals were housed in groups. All surgeries and other experimental procedures were in compliance with the standards of the Experimental Animal Center of Capital Medical University and the Beijing Experimental Animal Federation.

2.2. Preparation of the NT-3-chitosan implant

The chitosan tubes and NT-3-loaded chitosan carriers were fabricated under sterile conditions as previously described (Li et al., 2009a,b; Yang et al., 2010, 2015). After fabrication, the tubes were sterilized using 75% (vol/vol) alcohol and then washed with phosphate-buffered saline (PBS; 0.1 M, pH 7.4). Prior to implantation, 10 mg of chitosan carriers loaded with 100 ng NT-3 (Sigma-Aldrich) was injected into the middle of the tubes to obtain the C-NT3 implant.

2.3. Blinding the experimenters

The rats received a radio frequency identification (RFID) chip (Microchip ID Systems) prior to surgery by personnel from the Miami Project to Cure Paralysis. The treatments associated with the electronic ID of the rats remained concealed at the Miami Project to Cure Paralysis at the University of Miami during the entire survival period, behavioral assessments, electrophysiological measurements, and tissue processing.

2.4. Spinal cord transection and implantation

Rats were anesthetized using intraperitoneal injections of Equithesin (6.5 mg chloral hydrate and 3 mg sodium pentobarbital, 3 ml/kg; Sigma-Aldrich) and their back was shaved and aseptically prepared. A laminectomy of the 6th and 7th thoracic vertebrae was performed to expose the 7th and 8th thoracic spinal cord. A 5 mm long spinal cord segment was removed followed by complete aspiration of any residual tissue in the transection gap. Extra care was taken to remove all residual nervous tissue from the transection gap. Immediately after the lesion, rats received a chitosan tube filled with NT-3-loaded chitosan carriers (C-NT3; $n = 7$) or no implant (transection (T)-control; $n = 6$). The surgeons were unaware of the specific treatment for a given animal until the transection injury was completed. Other rats received a laminectomy of the 6th and 7th thoracic vertebrae but no transection (sham (*S*)-control; $n = 6$). After suturing the back muscles and the skin and disinfecting their backs, the rats recovered from anesthesia in a warmed environment after which they were returned to their cages. One rat died during the surgical procedures.

2.5. Post-surgery care and maintenance

Due to the strict blinding procedures, rats from different experimental groups were housed together, i.e., S-control rats were housed together with T-controls and/or C-NT3 rats. All rats received an intraperitoneal injection of penicillin (100,000 units) daily for 7 days post-surgery to prevent infections. Rats received subcutaneous injections of 20 ml of lactated Ringers' solution daily for 7 days to prevent dehydration. The bladders of the rats were emptied manually 3–4 times daily. Throughout survival, rats were monitored twice daily. Food and water were provided ad libitum. The post-surgery housing facility for the rats remained at 24–26 °C under 35–45% relative humidity and with a 12 h light/dark cycle. In total, 19 rats survived and were used for the experiment (Supplementary Table).

2.6. BrdU administration

To label proliferating cells, the rats received an intraperitoneal injection of 5-bromo-2-deoxyuridine (BrdU; 50 mg/kg in 0.9% NaCl; Sigma-Aldrich) once every 12 h for 7 days starting after surgery.

2.7. Hind limb motor function assessment

Hind limb movement of the rats ($n = 19$) was assessed at the end of the 3-month survival period using the Basso, Beattie and Bresnahan test (BBB; Basso et al., 1995, 1996). The assessments were recorded. Two groups of personnel at The Miami Project to Cure Paralysis and one group at Capital Medical University independently analyzed the video recordings of the hind limb movement assessments. There were no significant differences between the scores of the three groups.

2.8. Electrophysiological assessments

Rats ($n = 19$) were anesthetized using an intramuscular injection of ketamine (20 mg/kg body weight) and 6% chloral hydrate (0.2 ml/100 g) at 3-months post-surgery after the BBB test. Their hind limbs were gently fixed to a board with soft cloth loops. The room temperature was kept at 25–28 °C. The dual-channel mode of an electromyogram (Dantech) was used to detect motor-evoked potentials (MEPs) and somatosensory-evoked potentials (SEPs). For MEPs, the positive stimulating electrode (2 mm spherical) was placed on the skull surface at the midline of the cerebral cortex (A/P: −2.5 mm, ML: 2 mm, from Bregma), while the negative stimulating electrode (4 mm disk) was

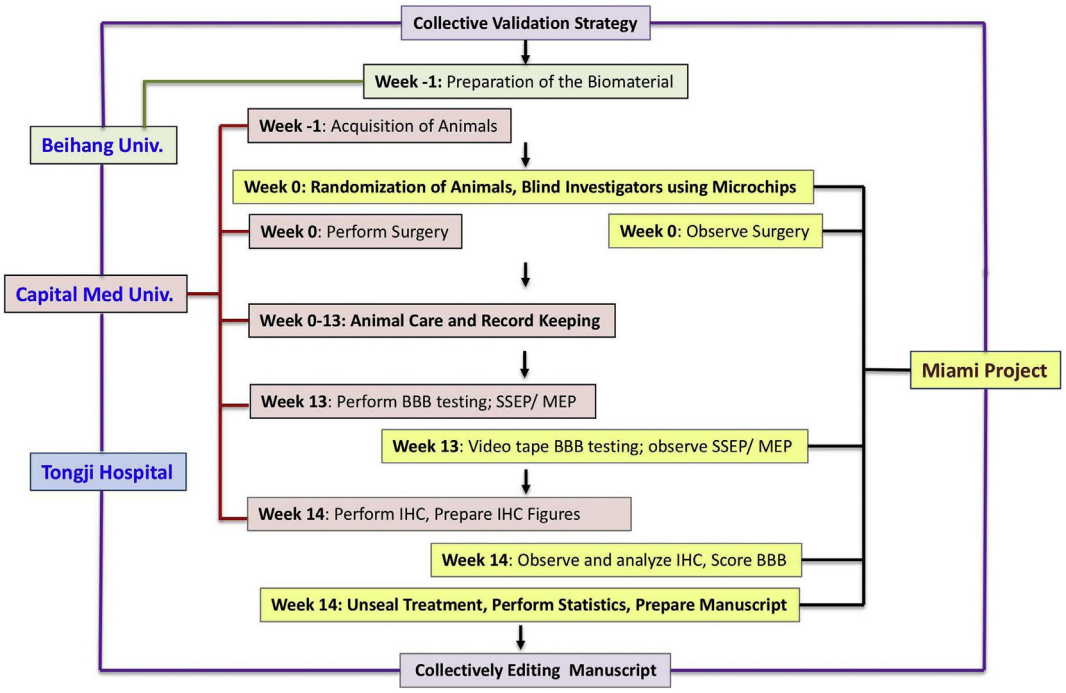

Fig. 1. *Schematic of the study design and blinding strategy.* The responsibilities of the team of researchers from The Miami Project are in yellow, those from Beihang University in green, and those from Capital Medical University in Beijing in purple and Tongji Hospital in blue. (For interpretation of the references to colour in this figure legend, the reader is referred to the web version of this article.)

placed on the nose above the hard palate skull surface (identical to Fig. 1D in Luo et al., 2018). Recording electrodes were placed in the tibialis anterior muscle in both hind limbs. The reference electrode was placed 2 cm from the distal end of the recording electrode. The ground wire was placed between the stimulating electrode and the recording electrode. A single square wave (10–15 mA, 0.2 s) at 1 Hz frequency (filter: 2–10 kHz; amplifier: 0.1 mV/D) was used to stimulate the motor area of the cerebral cortex and MEPs in both tibialis anterior muscles were recorded. We measured the time and amplitude from the negative peak to the adjacent positive peak as well as the distance between the stimulation and recording electrode. The MEPs were presented and statistically analyzed separately for the left and right limbs.

For SEPs, the positive stimulation electrodes were inserted into the tibialis anterior muscles in both hind limbs. Sustained 200 pulses (3–5 mA, 0.3 msec) at 20 Hz-3 kHz frequency (scan length: 80 msec, amplifier: 10 V/D) were given. With this approach, slight moving of the hind limb toes was observed. SEPs were recorded on the skull surface of the cerebral cortex sensory area, including P1 and P1-N1. The distance between the stimulating and recording electrodes was measured. The SEPs were presented and statistically analyzed separately for the left and right cortex.

2.9. Histology and immunocytochemistry

Rats were sedated as described above and transcardially perfused with 250 ml PBS (0.1 M, pH 7.4) followed by 400 ml 4% paraformaldehyde in PBS (0.1 M, pH 7.4). The spinal cord was removed from the vertebral column, kept in the same fixative for 6–8 h at 4 °C. Pictures of the transection/implant were taken using a dissecting microscope fitted with a camera. Then, a 1 cm long piece of the spinal cord centered on the transection/implant was embedded in paraffin and cut into 10 μm thick horizontal sections.

From 5 randomly selected rats from the T-control group and the C-NT3 group and 2 rats from the S-control group, sections were dewaxed, rehydrated, washed three times with 0.01 M PBS (pH 7.4), and incubated in a blocking solution (0.3% Triton X-100 with 10% normal goat serum) for 60 min at room temperature followed by the primary antibody for 60 h at 4 °C. We used primary rabbit polyclonal antibodies against nestin (1:100; Abcam ab93157) to recognize nestin-positive cells, βIII-tubulin (Tuj1, 1:400; Sigma T2200) to recognize immature neuron-like cells, NeuN (1:500; Abcam ab177487) to recognize mature neuron-like cells, and glial fibrillary acidic protein (GFAP, 1:300; Zymed) to detect astrocyte-like cells. We used mouse monoclonal antibodies to detect 5-bromo-2 -deoxyuridine (BrdU, 1:200; ZSGB Biotechnology ZM-0013) in cells that proliferated and neurofilament 200 kDa (NF-H, 1:200; Zymed ZM-0198) in axon-like processes. Sections stained for BrdU were first denatured with 2 N HCl at 37 °C for 30 min and then renatured with 0.1 M sodium tetraborate (pH 8.4) at 37 °C for 10 min. After incubation with the primary antibody, sections were washed three times in 0.01 M PBS (pH 7.4) and then incubated at room temperature for 1 h with fluorescein-conjugated secondary antibodies (1:300; Jackson Laboratory). Primary and secondary antibodies were diluted in 0.01 M PBS (pH 7.4). Finally, the sections were rinsed three times in 0.01 M PBS (pH 7.4) and covered with glass slips in antifading medium with DAPI (Vector Laboratories). All stained sections were scanned using a confocal microscope (TCS SP8, Leica, Germany). BrdU-positive cell was examined at full magnification using the *Z*-axis.

2.10. Statistical analysis

One-way ANOVA and Tukey post hoc test were used to statistically analyze group differences for MEPs and SEPs. The overground walking scores were statistically tested using the non-parametric Kruskal–Wallis H or Mann-Whitney *U* test (Prism 6.0 h). Differences were considered significant at $P < .05$.

3. Results

The original paper by Yang et al. (2015) investigated a number of different treatment conditions, where the C-NT3 implant was found to trigger neural tissue generation in the damaged spinal cord. At the 3-month time point, neural cells and axons were present in the tissue

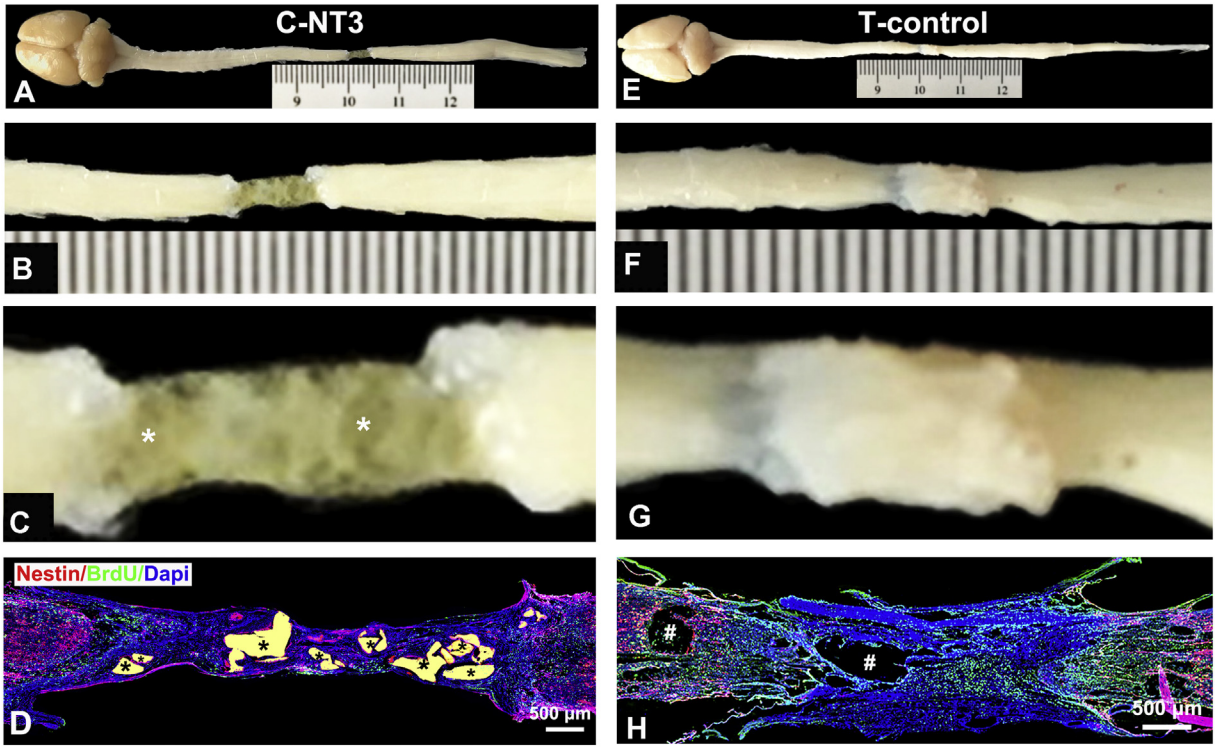

Fig. 2. *Gross morphology of the tissue cable in the transection gap.* In C-NT3 rats, a tissue cable was found spanning the transection gap (A). The cable had a smooth exterior (B, C), good apposition with the rostral and caudal spinal cord (C), and a diameter that was about 80% of that of the spinal cord (B, C). Chitosan carriers (asterisks) were visible in vivo (C) and in tissue sections (D). In T-control rats, a tissue cable was also present in the transection gap (E, F). This cable had a rough appearance (F, G) and a diameter that was larger than that of the spinal cord (G). Cavities were present in the tissue cable (H) as well as in the rostral and caudal spinal cord (number sign). Nestin immunoreactivity is present in the C-NT3 tissue cable (D) but not in the T-control (H).

bridge of C-NT3 treated animals in concert with electrophysiological signals and improvements in hind limb function (Yang et al., 2015). For the present validation study, we focused on those outcome measures in three key conditions: C-NT3, T-controls, and S-controls. We first present our anatomical results, followed by the data on behavior and electrophysiology, which may have been affected by changes in anatomy. The blinding strategy, the responsibility of the Miami Project to Cure Paralysis sub-group, and the design of this validation study are illustrated in Fig. 1.

3.1. A cellular tissue cable bridged the spinal cord transection gap

The dissected spinal cords were examined morphologically under a dissection microscope. In C-NT3 rats, a newly formed tissue cable was present spanning the entire 5-mm long transection gap connecting the rostral and the caudal spinal cord (Fig. 2A, B). The tissue cable had a smooth exterior with a yellow opaque appearance and with some visible chitosan carriers (Fig. 2C, D). In all but one rat, the width of the tissue cable was uniform across the transection gap with a diameter that varied 20–80% of the spinal cord. Some tissue cables contained cavities, which in some cases were also present in the rostral and caudal spinal cord nearby the tissue cable interface.

In T-control rats, tissue was present in the transection gap (Fig. 2E, F). This tissue had a rough appearance (Fig. 2F, G) with varying diameters compared with the cables in C-NT3 rats. In most cases, the diameter of the tissue appeared larger than that of the spinal cord (Fig. 2G). Many (DAPI-positive) cells were found in the tissue in the transection gap in T-control rats (Fig. 2H) compared with C-NT3 rats (Fig. 2D). This possibly reflects an influx of cells into the initially 'open' transection gap in T-control rats. More in depth analysis is necessary to determine the characteristics of these cells. Some of the tissue in T-control rats contained cavities (Fig. 2H) which were also present in the rostral and caudal spinal cord (Fig. 2H).

3.2. Nestin-, Tuj1-, and NeuN-positive cells were present in the C-NT3 tissue cable

We examined the tissue cables for the presence of nestin-positive cells using anti-nestin antibodies. DAPI was used to recognize nuclei and anti-BrdU antibodies to stain nuclei of cells that proliferated during the time of labeling. Nestin-positive cells were present in the interface of the C-NT3 tissue cable with the caudal and rostral (Fig. 3A-C) spinal cord in all animals examined. These regions also contained BrdU-positive nuclei (Fig. 3A-C) and nestin-/BrdU-double positive cells (Fig. 3D-F). The middle region of the tissue cable contained nestin-positive cells and BrdU-positive nuclei (Fig. 3G, H), but not nestin-/BrdU- double positive cells (Fig. 3I-K). We found ample nestin staining in both the rostral and caudal spinal cord near the interface with the tissue cable, especially around the central canal and in the white matter (Fig. 3A).

In T-control rats, BrdU-positive nuclei, but not nestin-positive cells, were observed throughout the tissue cable (Fig. 3L-N). In these rats, some nestin immunostaining was found around the central canal and in the white matter of the spinal cord rostral and caudal to the lesion (Fig. 3L). Our data support the possibility that nestin-positive cells, derived from the endogenous pool of NPCs, migrated from the spinal cord rostral and caudal to the lesion into the tissue cable in the C-NT3 implant.

The presence of neuron-like cells in the tissue cables was examined using antibodies against Tuj1 (Fig. 4) and NeuN (Fig. 5). DAPI was used to stain nuclei and antibodies against BrdU to stain the nucleus of cells that proliferated during the time of BrdU labeling. In C-NT3 rats, Tuj1-positive cells and BrdU-positive nuclei were observed in the interfaces of the tissue cable with the caudal and rostral (Fig. 4A-C) spinal cord. Tuj1-/BrdU-double positive cells were also found in these regions

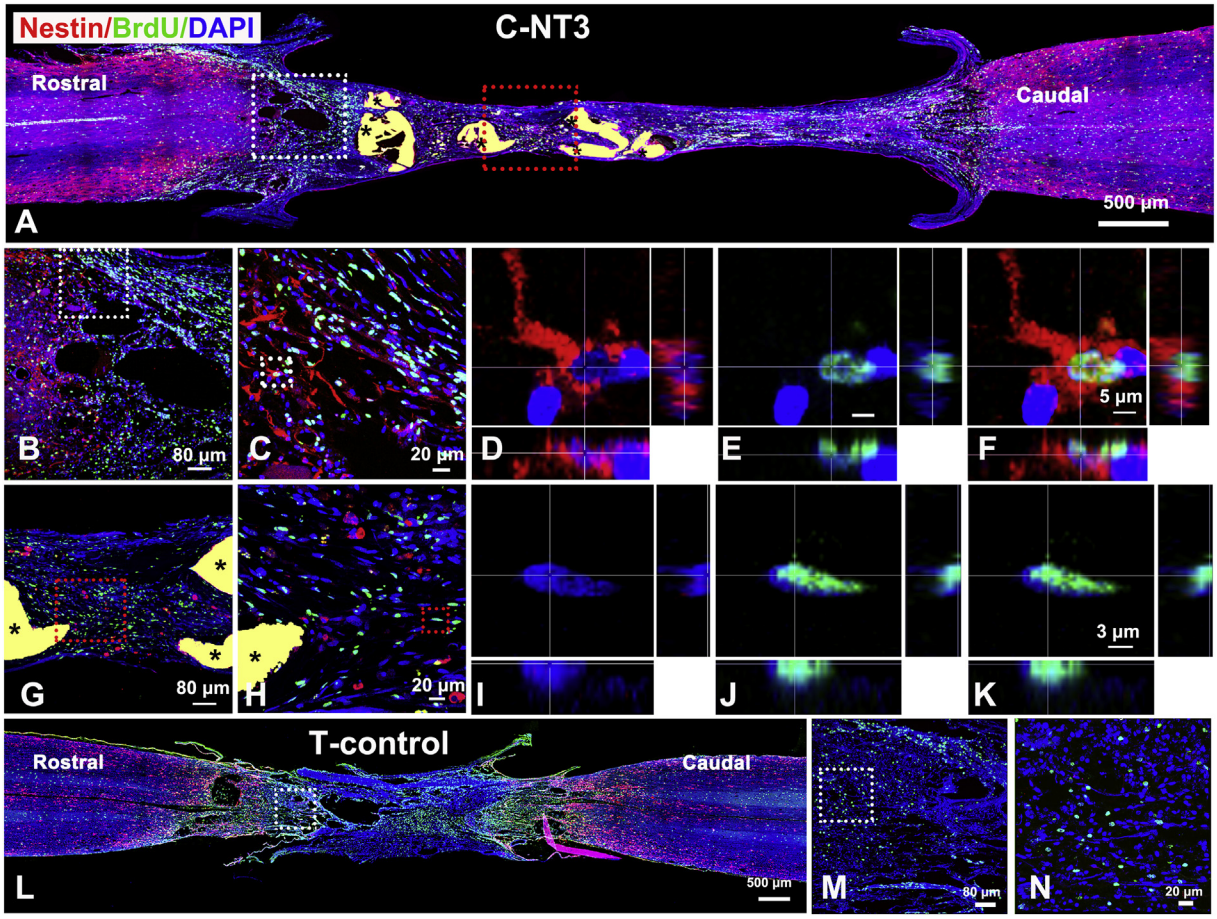

Fig. 3. *Cells expressing nestin were present in the tissue cable in C-NT3 rats but not T-control rats.* In C-NT3 rats, sections stained with antibodies against nestin and BrdU and counterstained with DAPI revealed the presence of nestin-positive cells in the interface of the tissue cable and the rostral spinal cord (A, white box). The area in the white box in A is magnified in panel B and the area in the white box in B is magnified in panel C. Some of the nestin-positive cells (D) had BrdU expressed within their nucleus (E). An example of a nestin/BrdU double expressing cell is depicted in panel F. Note that panels D–F depict the same cell. Nestin- and nestin/BrdU-positive cells were also present in the interface of the tissue cable and the caudal host spinal cord (not shown). Areas more towards the middle of the tissue cable contained cells with a BrdU-positive nucleus (A, red box) which are depicted in higher magnification in panel G (magnification of red box in panel A) and H (magnification of red box in panel G). The cells in panels I, J, and K (magnification of red box in panel H) did not necessarily stain positive for nestin (I) but clearly contained BrdU in their nucleus (J). An example of a nestin-negative/BrdU-positive cell is depicted in panel K. Note that panels I–K depict the same cell. Nestin was expressed in the rostral and caudal spinal cord near the interface with the tissue cable (A). In the tissue cable in T-control rats, cells with a BrdU-positive nucleus were present but no cells that expressed nestin (L). The area in the white box in L is magnified in panel M and the area in the white box in M is magnified in panel N. Some nestin expression was observed in the rostral and caudal host spinal cord near the interface with the tissue cable. (For interpretation of the references to colour in this figure legend, the reader is referred to the web version of this article.)

(Fig. 4D-F). Similarly, Tuj1-positive cells (Fig. 4L, M), BrdU-positive nuclei (Fig. 4G, H), and Tuj1-/BrdU-double positive cells (Fig. 4I-K) were found in regions closer to the middle of the tissue cable. Tuj1 immunostaining was found in the gray and white matter in the spinal cord rostral and caudal to the tissue cable (Fig. 4A). In T-control rats, Tuj1-positive cells were not detected in the tissue cables in the transection gap (Fig. 4L-N). Tuj1-positive cells were detected in the spinal cord rostral and caudal to the tissue cable (Fig. 4L). These staining patterns were indicative of neurogenesis occurring after implantation of the C-NT3 implant and resulting in the presence of Tuj1-positive, Tuj1/BrdU double positive newborn neurons (or neuron-like cells) in the tissue cable.

NeuN-positive cells and BrdU-positive nuclei were detected in the caudal and rostral (Fig. 5A-C) region of the tissue cable. NeuN-/BrdU-double positive cells were also found in these regions (Fig. 5D-F). In the middle of the tissue cable, NeuN-positive cells (Fig. 5G, H), BrdU-positive nuclei (Fig. 5G, H), and NeuN-/BrdU-double positive cells (Fig. 5I-K) were detected. In the rostral and caudal spinal cord near the interfaces with the tissue cable, ample NeuN immunostaining was found in the gray matter (Fig. 5A). In T-control rats, NeuN expression was not detected in the tissue cable in the transection gap (Fig. 5L-N). BrdU-positive nuclei were found in this newly formed tissue (Fig. 5M, N). NeuN immunostaining was found in the gray matter in the rostral and caudal spinal cord (Fig. 5L). These data suggested that some cells had migrated from the spinal cord into the tissue cable in the C-NT3 implant and differentiated into NeuN-positive and/or NeuN-/BrdU-double positive newborn neurons (or neuron-like cells).

3.3. NF- and GFAP-positive processes were present in the tissue cable in C-NT3 implanted rats

We examined the tissue cables after staining with antibodies directed against NF and GFAP. DAPI was used to stain nuclei. In rats with the C-NT3 implant, NF-positive processes were present in the caudal and rostral (Fig. 6A-C) aspect of the tissue cable near the interface with the spinal cord. These NF-positive profiles were often associated with GFAP-positive processes (Fig. 6C-E). Centrally in the tissue cable, we detected NF-positive processes (Fig. 6F, G) but not GFAP-positive processes (Fig. 6H, I). In the rostral and caudal spinal cord, adjacent to the tissue cable, abundant NF and GFAP immunostaining was observed

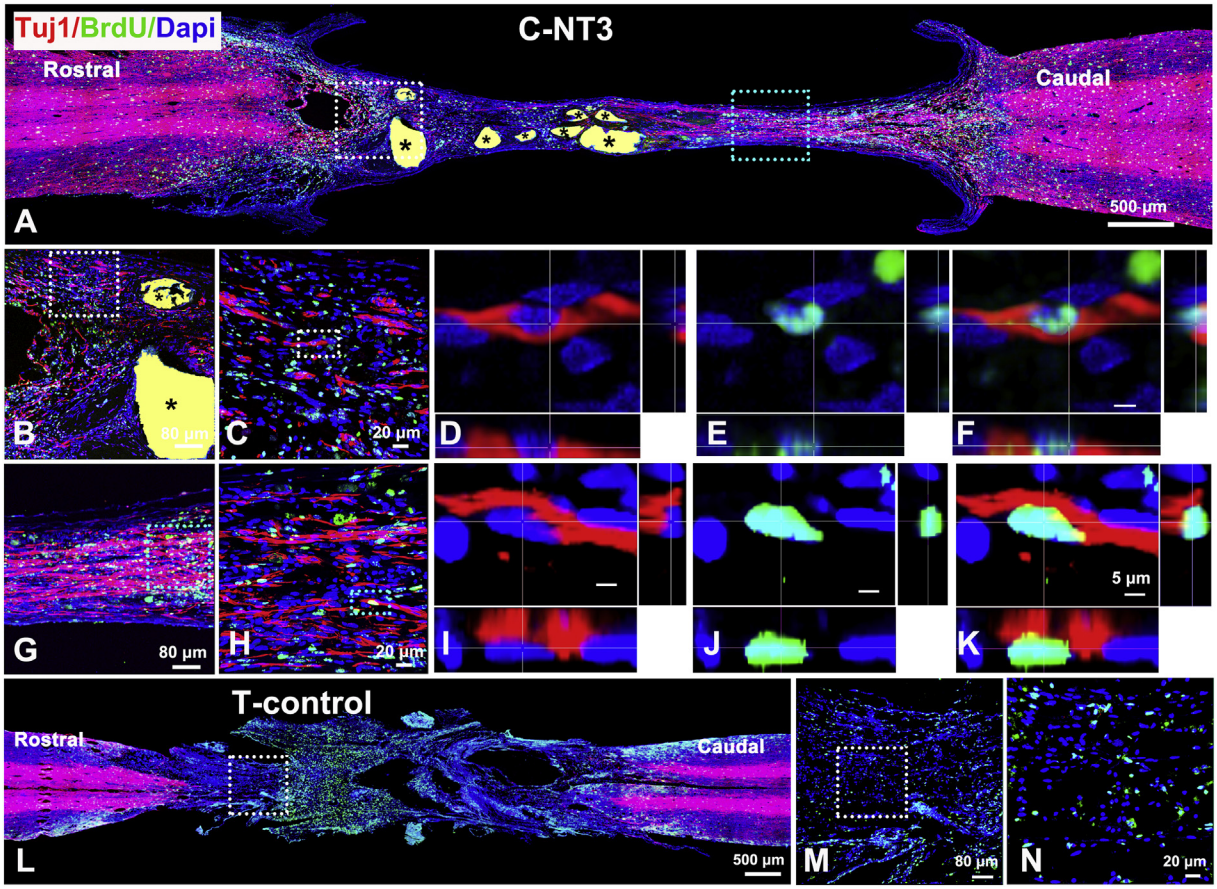

Fig. 4. *Tuj1-positive cells were present in the tissue cable in C-NT3 but not T-control rats.* In C-NT3 rats, sections stained for Tuj1 and BrdU and counterstained with DAPI revealed that Tuj1-positive cells were present in the interface of the tissue cable and the rostral spinal cord (A, white box). These cells are shown in higher magnification in panel B (magnification of area in white box in A) and panel C (magnification of area in white box in B). Some of the Tuj1-positive cells (D) had a BrdU-positive nucleus (E). An example of such Tuj1/BrdU-positive cells is provided in panel F. Note that panels D-F depict the same cell. Tuj1-positive cells were also present in the interface of the tissue cable and the caudal spinal cord (not shown). Areas towards the middle of the tissue cable contained Tuj1-positive cells (A, blue box). A closer view of these cells is provided in panel G (magnification of area in blue box in A) and in panel H (magnification of area in blue box in G). Tuj1-positive cells (I) often had a BrdU-positive nucleus (J). An example of a Tuj1/BrdU-positive cells is shown in panel K. Note that panels I–K depict the same cell. Tuj1 staining was present in white and gray matter in the rostral and caudal spinal cord near the interface with the tissue cable (A). In T-control rats, the tissue cable contained cells with a BrdU-positive nucleus but no cells that expressed Tuj1 (L). A closer view of these cells is provided in panel M (magnification of area in white box in L) and in panel N (magnification of area in white box in M). In T-control rats, Tuj1 staining was found in the rostral and caudal spinal cord near the interface with the tissue cable (L). (For interpretation of the references to colour in this figure legend, the reader is referred to the web version of this article.)

(Fig. 6A). In T-control rats, few NF-positive processes were found near the interface of the tissue cable and the caudal and rostral (Fig. 6J-L) spinal cord. Some GFAP-positive processes were also found in these regions (Fig. 6M, N). In regions closer to the middle of the tissue cable, neither NF-positive (Fig. 6O, P) nor GFAP-positive processes (Fig. 6Q, R) were observed. These results indicated that NF-positive, axon-like processes and GFAP-positive, astrocyte-like processes had grown into the tissue cable that had generated in the C-NT3 implant.

3.4. Overground walking performance

Hind limb movement was assessed using the BBB test (Basso et al., 1995, 1996). The BBB scores of the left and right limb were mostly similar (Fig. 7A) and therefore averaged to assign one score per rat (Fig. 7B). The BBB score of the C-NT3 group was 2.0 ± 2.3 (mean ± SD; Fig. 7B), indicating extensive movement of one joint or extensive movement of one joint and slight movement of one other joint. In this group, 1/7 rats was flaccid; 3/7 rats showed slight movement of a joint in one or both hind limbs; 1/7 rats had slight movements of all three joints in both hind limbs; 1/7 rats showed slight movements of 2 joints and extensive movement of the third joint in one hind limb, while the other limb was flaccid; 1/7 rats had extensive movement of one joint and slight movement in the two other joints in one hind limb, while the other limb showed extensive in two joints and slight movement in the third joint. The non-responder in this group had a large cavity in the rostral spinal cord near the interface with the tissue cable, which was rather thin especially at the caudal aspect (See Supplementary Figure). The BBB score of the T-control group was 0.1 ± 0.3 (mean ± SD; Fig. 7B), indicating flaccid hind limbs. In this group, 1/6 rats had slight movement of one joint. The BBB score for the S-control group was 20.8 ± 0.9 (mean ± SD; Fig. 7B), indicating normal walking behavior with consistent plantar stepping and coordinated gait, consistent toe clearance, predominant parallel paw positioning throughout stance, consistent trunk stability, and tail consistently up. In 1/6 rats we found that the predominant paw positioning was parallel at the initial contact and rotated at lift off. Statistical evaluation showed that the BBB score of the C-NT3 group was significantly larger than that of the T-control group ($p < .05$; Fig. 7B). The Beijing Capital Medical University group also performed BBB scoring on the behavioral videos (Supplementary Table). The results from independent scoring from the two institutions were slightly variable but in general agreement with each other.

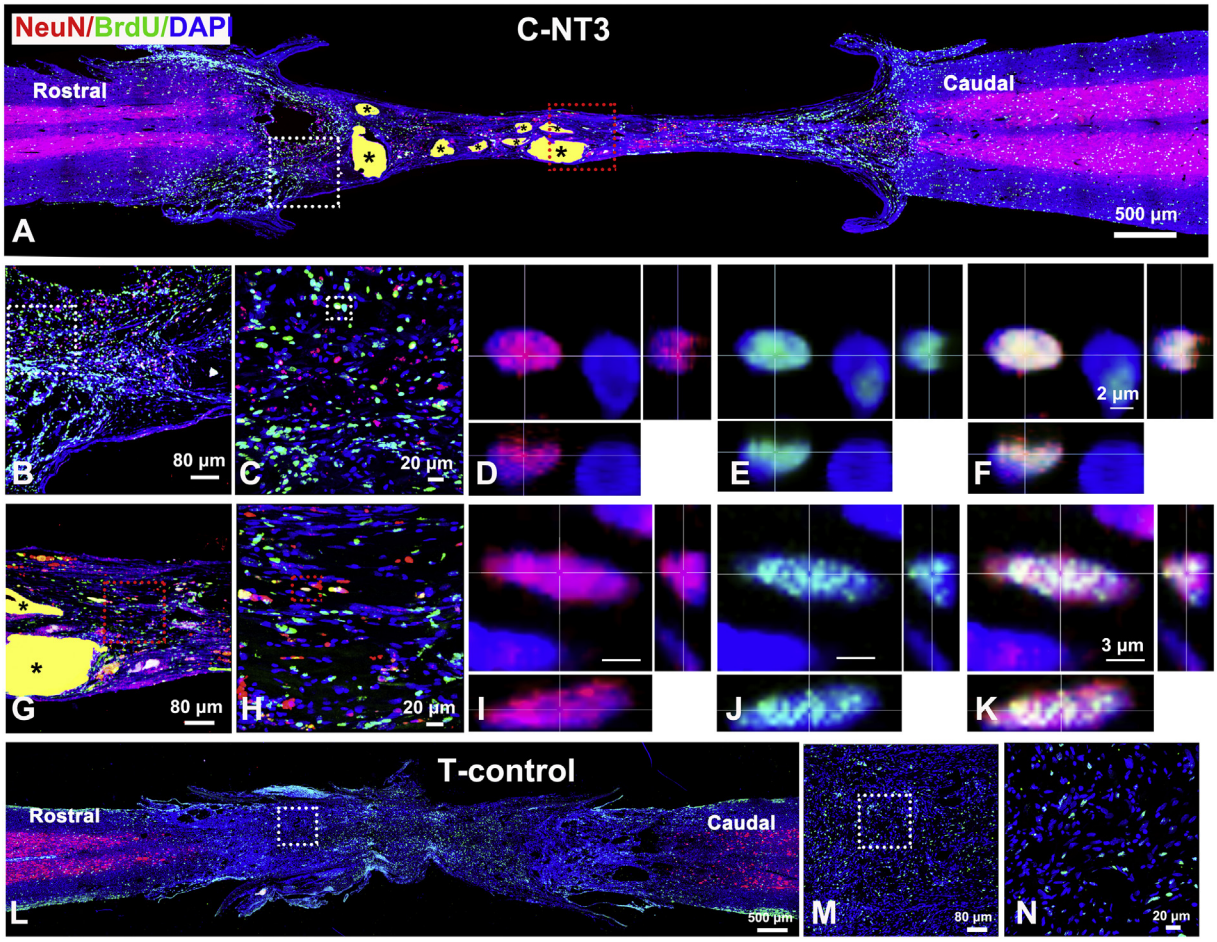

Fig. 5. *Cells expressing NeuN were present in the tissue cable in C-NT3 but not T-control rats.* In C-NT3 rats, sections stained for NeuN and BrdU and counterstained with DAPI revealed the presence of NeuN-positive cells in the interface of the tissue cable and the rostral spinal cord (A, white box). A magnification of the area in the white box in panel A is shown in panel B and a magnification of the area in the white box in panel B in panel C. Some NeuN-positive cells (D) had a BrdU-positive nucleus (E). An example of a NeuN/BrdU-positive cell is shown in panel F. Note that panels D-F depict the same cell. NeuN- and NeuN/BrdU-positive cells were also present in the interface of the tissue cable and the caudal spinal cord (not shown). Areas in the middle of the tissue cable contained NeuN/BrdU-positive cells (A, blue box). Panel G provides a magnification of the area in the red box in A and panel H provides a magnification of the area in the red box in G. The NeuN-positive cells (I) often had a BrdU-positive nucleus (J). An example of a NeuN/BrdU-positive cell is shown in panel K. Note that panels I–K depict the same cell. NeuN staining was present in gray matter in the rostral and caudal spinal cord (A). In T-control rats, the tissue cable contained cells with a BrdU-positive nucleus but no cells expressing NeuN (L). The area in the white box in L is magnified in panel M and the boxed area in M is magnified in panel N. In T-control rats, NeuN staining was found in the gray matter in the rostral and caudal host spinal cord (L). (For interpretation of the references to colour in this figure legend, the reader is referred to the web version of this article.)

3.5. Electrophysiological measurements

Motor-evoked potentials (MEPs) were elicited in the tibialis anterior muscles of the left and right hind limbs after stimulation of the contralateral sensorimotor cortices and latencies and amplitudes were determined (Fig. 8A). Examples of raw data of rats representing the three experimental groups are provided (Fig. 8B); there were no asymmetries observed. MEPs were recorded from tibialis anterior muscles in C-NT3 rats but not in T-control rats. The amplitudes of C-NT3 MEPs were significantly smaller than those in S-control rats in both left ($p = .07$) and right ($p = .014$) hind limb (Fig. 8C). The latencies of the MEPs in C-NT3 rats were not different from those recorded in S-control rats in the left hind limb ($p = .2$), but significantly longer in the right hind limb ($p = .001$; Fig. 8D).

Somatosensory-evoked potentials (SEPs) were elicited in the left and right sensorimotor cortices after stimulation of the contralateral tibialis anterior muscles and latencies and amplitudes were measured (Fig. 8A). Examples of raw data of animals representing the three experimental groups are provided (Fig. 8E). There were no asymmetries observed in the recorded data. SEPs were recorded from the sensorimotor cortices of C-NT3 rats but not detected in T-control rats. The amplitudes of C-NT3 SEPs were significantly smaller than those recorded in S-control rats from the left cortex ($p < .001$) but not the right cortex ($p = .16$; Fig. 8F). The latencies of the SEPs in C-NT3 rats were not different from those recorded in S-control rats from either the left or right cortex ($p > .7$; Fig. 8G).

4. Discussion

Generating new neural tissue in the damaged spinal cord may provide a foundation for repair and recovery (Chen, 2014). It was previously shown that implantation of a chitosan tube holding chitosan carriers releasing NT-3 (C-NT3 implant) into complete transected adult rat spinal cords resulted in anatomical repair and functional recovery (Yang et al., 2015). Here, we aimed to validate the results from Yang and colleagues using three important treatment groups at the 3-month time point by comparing anatomical, electrophysiological, and behavioral outcomes in rats after complete transection. In C-NT3 rats, a tissue cable was present in the transection gap containing neuron-like cells and axon- and astrocyte-like processes at 3-months after surgery

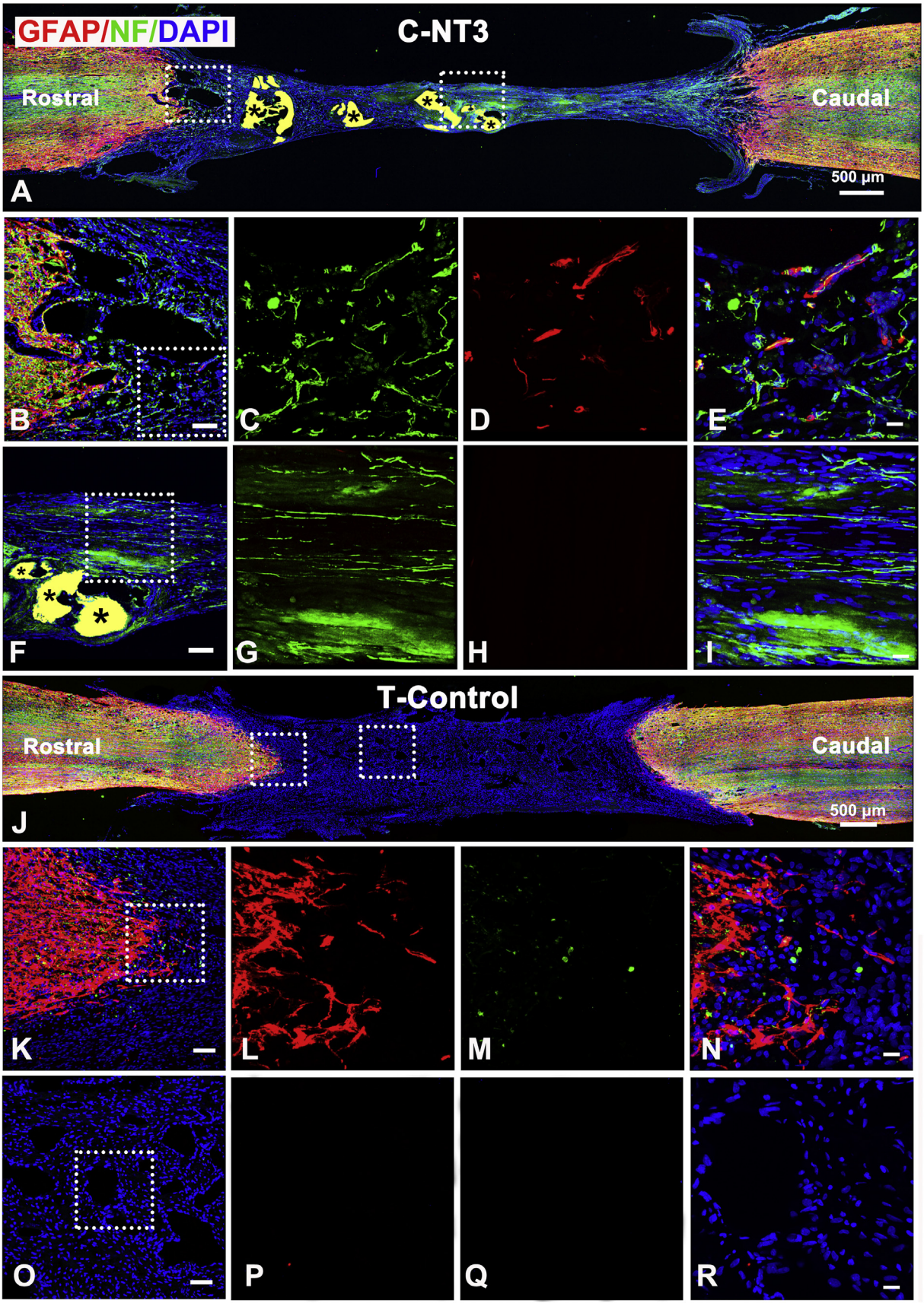

(caption on next page)

Fig. 6. *NF-positive processes were detected in the tissue cable of C-NT3 but not T-control.* In C-NT3 rats, sections stained for GFAP and NF and counterstained with DAPI showed GFAP- and NF-positive processes in the interface of the tissue cable and the rostral spinal cord (A). A magnification of the area in the white box in panel A near the rostral interface is provided in panel B. The area in the white box in panel B is magnified to show NF-positive processes (C), GFAP-positive processes (D), and NF- and GFAP-positive processes (E). GFAP- and NF-positive processes were also present in the interface of the tissue cable and the caudal host spinal cord (not shown). In the middle of the tissue cable NF-positive processes were present (A, F). The white box in panel F is magnified to show NF-positive axons (G) and the absence of GFAP staining (H). Panel I shows the boxed area in panel F double stained for GFAP and NF revealing the presence of NF- and absence of GFAP-positive processes. In T-control rats, the tissue cable contained a few GFAP-positive processes near the interfaces (J). The area in the white box in the rostral interface is magnified in panel K. The area in the white box in panel K is magnified to show GFAP-positive processes (L), NF-positive processes (M) and both NF and GFAP-positive processes (N). Areas deeper into the tissue cable (J, O) did not contain any NF- or GFAP-positive profiles. The area in the white box in panel O is magnified to more clearly show the absence of GFAP-positive profiles (P), NF-positive profiles (Q), or both (R). In T-control rats, NF and GFAP staining was present throughout the rostral and caudal spinal cord (J).

and implantation. In C-NT3 rats, MEPs in the tibialis anterior and SEPs in the motor cortex were recorded after stimulation of the motor cortex and tibialis anterior, respectively. Hind limb movement was improved in C-NT3 rats compared with transection only rats (T-controls). Our data indicated that the chitosan-based NT-3-releasing implant elicits endogenous neurogenesis. Moreover, we validated the potential of this particular implant for tissue generation in the injured spinal cord.

The tissue cable that formed in the C-NT3 rats, but not T-controls, contained nestin-, Tuj1-, and NeuN-positive cells. Cells positive for nestin, a marker for NPCs (Dahlstrand et al., 1995), were found at the rostral and caudal ends of the new tissue cable and some co-localized with BrdU. These findings support the possibility that newly born NPCs had migrated into the tissue generated in the C-NT3 implant from both the rostral and caudal direction. Cells positive for Tuj1, a marker for immature neuron-like cells (Thomas et al., 1996), or NeuN, a marker for mature neuron-like cells (Mullen et al., 1992), were present throughout the tissue cable. The presence of Tuj1- and NeuN-positive cells, but not nestin-positive cells, in the middle of the tissue cable may reflect that differentiation into neurons takes place during migration further into the tissue cable. Overall, our data suggest the occurrence of neurogenesis in C-NT3 rats with the resulting cells becoming part of the cytoarchitecture of the newly modeled tissue.

In rats with and without the C-NT3 implant, cavities were found in the tissue spanning the transection gap. The tissue cable in the T-control rats had more and larger cavities compared with those in the C-NT3 rats. Typically, cavities can be found in the newly generated tissue, transplanted tissue, and in the spinal cord close to the injury site (Hagg and Oudega, 2006; Ahuja et al., 2017). In the present study, it is also possible that cavities in the tissue cable in C-NT3 rats were formed when some of the remaining chitosan chips, that clearly had not yet completely degenerated, fell out during the histological processing. In the T-control rats, cavities may have resulted from an incomplete formation of the tissue cable, in which neurogenesis did not appear to play a role.

Our findings are fundamentally in agreement with Yang et al. (2015) who used a C-NT3 implant in the same adult rat SCI model. Similar as observed in the present study, Yang and co-workers (2015) described a tissue cable with similar anatomical features bridging the transection gap and connecting the spinal cord stumps at 3-months after implantation. Their results also indicated a bi-directional neurogenesis response resulting in neural cells present throughout the tissue cable as was suggested by the results in the present study. Yang et al. (2015) demonstrated the crucial role of NT-3 in the neurogenesis response elicited after implantation of the C-NT3 implant; however, their neurogenic response at 3 months post-implantation seemed more abundant compared with the present study. It is possible that differences in the amount or release kinetics of the NT-3 chitosan carriers influenced the migration and differentiation of local NPCs. The precise role of chitosan that carries NT-3 in neurogenesis remains to be elucidated.

The tissue cable in C-NT3 rats contained NF-positive processes in its rostral and caudal aspect, suggesting ingrowth of axons from the spinal cord into the tissue cable. Many of these were associated with GFAP-positive processes, which most likely were derived from astrocytes located in the adjacent spinal cord. It is possible that the astrocytic processes supported and guided the ingrowth of the axons, which was previously shown to occur into a Schwann cell cable in an adult rat model of a complete spinal cord transection (Williams et al., 2015). In some of the rats with the C-NT3 implant, the axons had reached as far

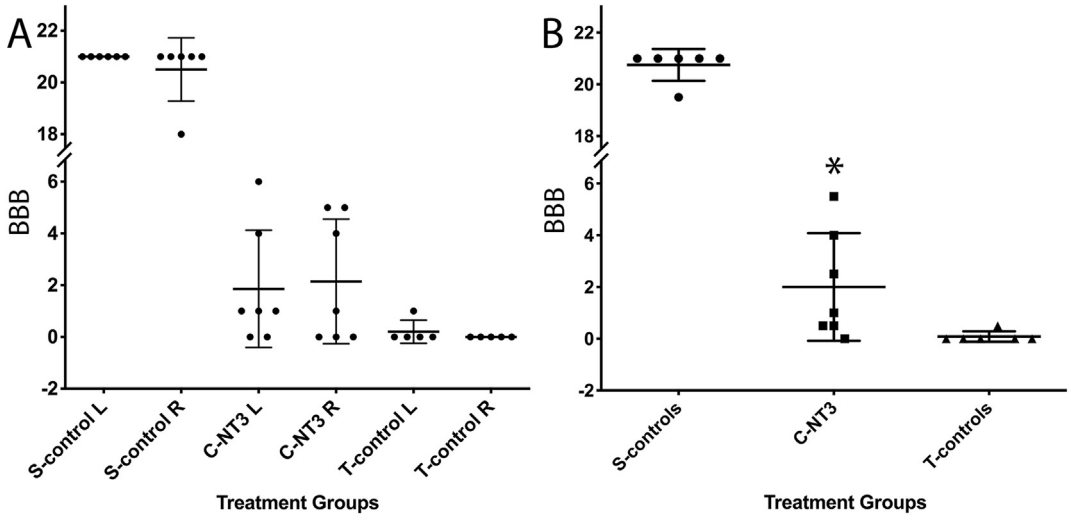

Fig. 7. *Overground walking performance was improved in rats with the C-NT3 implant compared with no implant.* Scatter dot plots showing that the average BBB score of the left hind limb in C-NT3 rats were significantly higher than that in T-control rats (A). Similarly, the average BBB score of the right limb in C-NT3 rats was significantly higher than that in T-control rats (A). The average BBB scores of the left and right hind limb in S-control rats that received a laminectomy only (A) were not significantly different from normal uninjured rats that have a score of 21. Scatter dot plots showing that when BBB scores were averaged for the left and right hind limbs, similar statistical differences were found between the three groups (B).

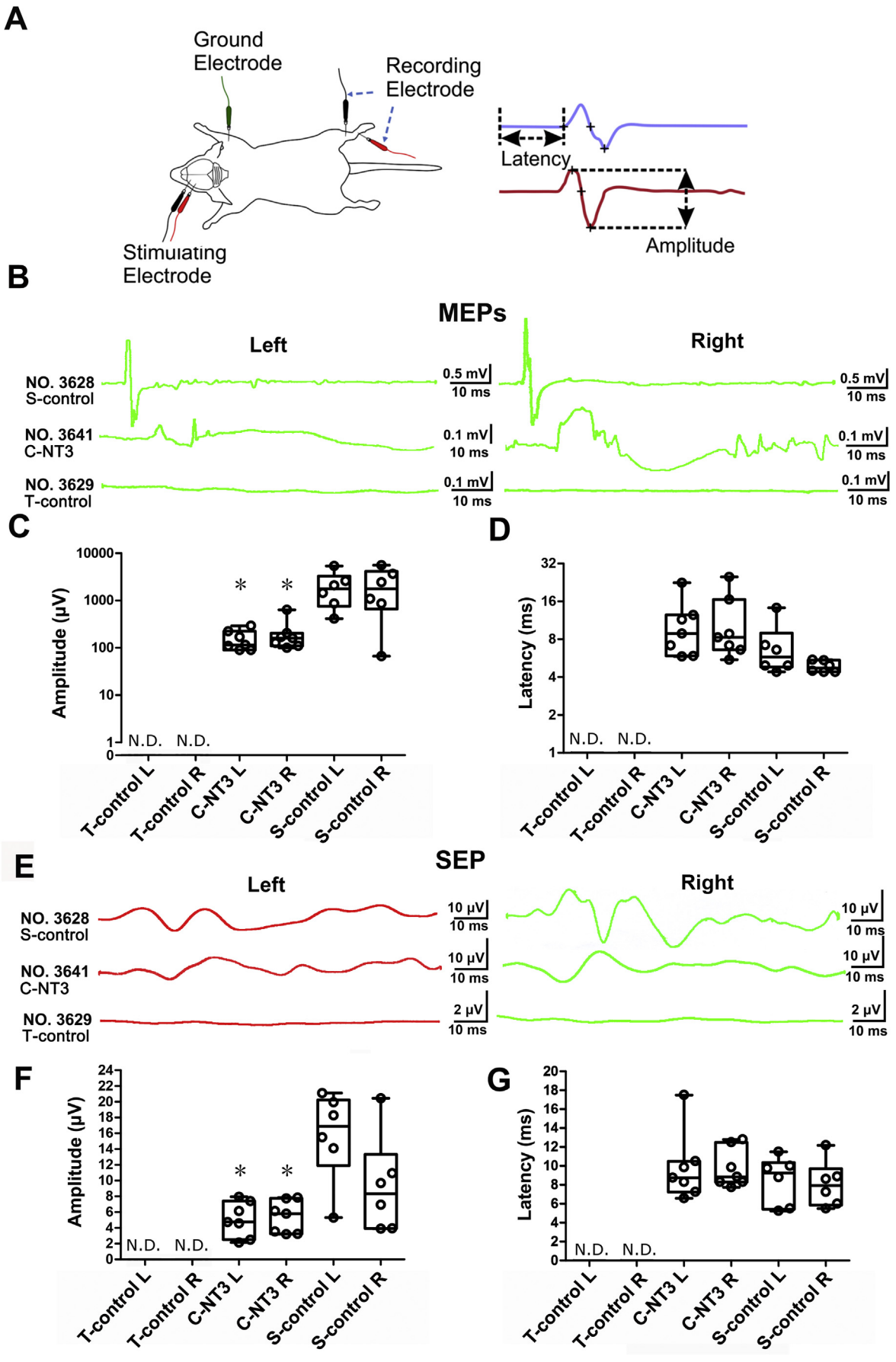

(caption on next page)

Fig. 8. *MEPs and SEPs were detected in rats with the C-NT3 implant but not in T-control rats.* (A) Schematic representation of the experimental set-up for stimulation and measuring MEPs and SEPs and for the calculation of the latency and amplitude of the recorded signals. (B) Examples of raw data of MEP recordings from the left and right hind limb from a rat from each of the three experimental groups (rat 3628, S-control group; rat 3641, C-NT3 group); rat 3629, T-control group). Boxplots showing the average amplitude (C) and latency (D) of the MEPs recorded from the left and right hind limb. The amplitudes from the signals from each hind limb recorded from C-NT3 rats were significantly lower than those from S-control rats (C). There were no statistical differences (D) between the latency of the signals from both hind limbs in C-NT3 and S-control rats. (E) Examples of raw data of SEP recordings from the left and right cortex in a rat from each of the three experimental groups (rat 3628, S-control group; rat 3641, C-NT3 group); rat 3629, T-control group). Boxplots showing the average amplitude (F) and latency (G) of the MEPs recorded from the left and right hind limb. The amplitudes from the signals from each cortex recorded from C-NT3 rats were significantly lower than those from S-control rats (F). There were no statistical differences (G) between the latency of the signals from both hind limbs in C-NT3 and S-control rats.

as in the middle of the tissue cable. In contrast, in all T-control rats, the growth response was less and processes had not extended beyond the rostral and caudal aspect of the tissue cable. Possibly, the neurotropic actions of NT-3 released from the chitosan carriers had elicited a more pronounced growth response. These growth responses in C-NT3 rats described here were similar to that reported by Yang et al. (2015).

In rats with the C-NT3 implant, but not in T-controls, MEPs were elicited in the tibialis anterior after stimulation of the motor cortex and SEPs were present in the sensorimotor cortex after stimulation of the tibialis anterior. These MEPs and SEPs had similar latencies and smaller amplitudes than those in S-control, which received a laminectomy only. Our electrophysiological findings suggest the presence of a neural circuitry connecting the hind limbs and the cortex. Previously, observations by Yang et al. (2015) suggested the presence of such connections in adult rats from 1 month after implantation of a C-NT3 implant in the complete transected spinal cord. Studies using trans-synaptic neuronal and axonal tracers, such as the rabies parvo virus (Dum and Strick, 2013), could possibly shed light on the existence of cortical-tibialis anterior axonal connections in rats with a C-NT3 implant in the transected spinal cord.

Hind limb movement in C-NT3 rats was improved compared with that in T-control. A significant correlation was found between hind limb movement and MEP amplitude and SEP latency and amplitude. The improvement in hind limb movements in this study was less than that observed at the 3-month time point in the study by Yang et al. (2015). There are several plausible explanations for this difference between the two studies. The rats in the current study were tested only at the 3-month time point, while the rats in the previous study were tested weekly after implantation of the scaffold. The presence of novel observers (from Miami) and changes in vivarium procedures (due to renovations) (Basso et al., 1995) may have influenced the performance of the rats during testing. An alternative explanation may be that in the present study the newly formed tissue cable matured slower that in the study by Yang et al. (2015), which was suggested by our anatomical and cellular observations, possibly due to differences in NT-3 release from the implant. This possibility that the release of NT-3 determines tissue maturation during the healing process needs to be investigated in future studies.

In the present study, we used female rats only because this reproduced what was done in the original study by Yang et al. (2015) which we aimed to validate here. In future experiments, female and male rats should be used to better represent the SCI population.

It is worth noting that this validation study achieved success on the very first attempt, with no optimization of the coordination of the two teams, animal care procedures, and behavioral assays. Given the fact that SCI studies are especially difficult to reproduce (Steward et al., 2012), confirming the finding that the C-NT3 implant elicited neurogenesis associated with electrophysiological signals and hind limb function improvements supports the potential of the C-NT3 implant for treatment of SCI.

Acknowledgments

We thank the Beihang University and Capital Medical School for their support in performing the experiments and the Tongji Hospital for funding the participation of members of The Miami Project to Cure Paralysis and the Animal Core Facility of The Miami Project for assessing overground walking. We thank Dr. Alejandro Mantero of the U.M. Biostatistics Collaboration and Consulting Core for advice on statistics. We thank Dr. Thomas Sudhof for his advice in the early planning of the validation study. VPL, YES, ZY, LC and XL conceived the project. MO, DJL, VPL, YS, YES, and HD contributed to the experimental design. XL prepared the biomaterials. DJL, VPL, YS blinded other investigators to treatments. JS, HD, PH, ZW, JS, YS, DJL, MO, VPL participated in the experiments. MO, AEH, DJL, VPL participated in analyzing and statistically testing the data. MO, DJL, VPL, AEH, YES participated in drafting the manuscript. JS, PH, YS, HG, ZY, LC, XL, YES edited the manuscript. VPL holds the Walter G. Ross Distinguished Chair in Developmental Neuroscience.

Declarations of interest

DJL, VPL, YS received honoraria and travel expenses from Beihang University to participate in this study.

References

Ahuja, C.S., Nori, S., Tetreault, L., Wilson, J., Kwon, B., Harrop, J., Choi, D., Fehlings, M.G., 2017. Traumatic spinal cord injury-repair and regeneration. Neurosurgery 80 (3S), S9–S22.

Alonso, G., 1999. Neuronal progenitor-like cells expressing polysialylated neural cell adhesion molecule are present on the ventricular surface of the adult rat brain and spinal cord. J. Comp. Neurol. 414 (2), 149–166.

Barnabé-Heider, F., Göritz, C., Sabelström, H., Takebayashi, H., Pfrieger, F.W., Meletis, K., Frisén, J., 2010. Origin of new glial cells in intact and injured adult spinal cord. Cell Stem Cell 7 (4), 470–482.

Basso, D.M., Beattie, M.S., Bresnahan, J.C., 1995. A sensitive and reliable locomotor rating scale for open field testing in rats. J. Neurotrauma 12 (1), 1–21.

Basso, D.M., Beattie, M.S., Bresnahan, J.C., 1996. Graded histological and locomotor outcomes after spinal cord contusion using the NYU weight-drop device versus transection. Exp. Neurol. 139 (2), 244–256.

Begley, C.G., Ellis, L.M., 2012. Drug development: raise standards for preclinical cancer research. Nature 483 (7391), 531–533.

Button, K.S., Ioannidis, J.P., Mokrysz, C., Nosek, B.A., Flint, J., Robinson, E.S., Munafo, M.R., 2013. Power failure: why small sample size undermines the reliability of neuroscience. Nat. Rev. Neurosci. 14 (5), 365–376.

Callahan, A., Anderson, K.D., Beattie, M.S., Bixby, J.L., Ferguson, A.R., Fouad, K., Jakeman, L.B., Nielson, J.L., Popovich, P.G., Schwab, J.M., Lemmon, V.P., Participants, F.S.W., 2017. Developing a data sharing community for spinal cord injury research. Exp. Neurol. 295, 135–143.

Chen, T.H., 2014. Tissue regeneration: from synthetic scaffolds to self-organizing morphogenesis. Curr Stem Cell Res Ther 9 (5), 432–443.

Dahlstrand, J., Lardelli, M., Lendahl, U., 1995. Nestin mRNA expression correlates with the central nervous system progenitor cell state in many, but not all, regions of developing central nervous system. Brain Res. Dev. Brain Res. 84 (1), 109–129.

Dum, R.P., Strick, P.L., 2013. Transneuronal tracing with neurotropic viruses reveals network macroarchitecture. Curr. Opin. Neurobiol. 23 (2), 245–249.

Gage, F.H., 2000. Mammalian neural stem cells. Science 287 (5457), 1433–1438.

Hagg, T., Oudega, M., 2006. Degenerative and spontaneous regenerative processes after spinal cord injury. J. Neurotrauma 23 (3–4), 264–280.

Kwon, B.K., Soril, L.J., Bacon, M., Beattie, M.S., Blesch, A., Bresnahan, J.C., Bunge, M.B., Dunlop, S.A., Fehlings, M.G., Ferguson, A.R., Hill, C.E., Karimi-Abdolrezaee, S., Lu, P., McDonald, J.W., Muller, H.W., Oudega, M., Rosenzweig, E.S., Reier, P.J., Silver, J., Sykova, E., Xu, X.M., Guest, J.D., Tetzlaff, W., 2013. Demonstrating efficacy in preclinical studies of cellular therapies for spinal cord injury - how much is enough? Exp. Neurol. 248, 30–44.

Landis, S.C., Amara, S.G., Asadullah, K., Austin, C.P., Blumenstein, R., Bradley, E.W., Crystal, R.G., Darnell, R.B., Ferrante, R.J., Fillit, H., Finkelstein, R., Fisher, M., Gendelman, H.E., Golub, R.M., Goudreau, J.L., Gross, R.A., Gubitz, A.K., Hesterlee, S.E., Howells, D.W., Huguenard, J., Kelner, K., Koroshetz, W., Krainc, D., Lazic, S.E., Levine, M.S., Macleod, M.R., McCall, J.M., Moxley 3rd, R.T., Narasimhan, K., Noble, L.J., Perrin, S., Porter, J.D., Steward, O., Unger, E., Utz, U., Silberberg, S.D., 2012. A

call for transparent reporting to optimize the predictive value of preclinical research. Nature 490 (7419), 187–191.
Lazic, S.E., Essioux, L., 2013. Improving basic and translational science by accounting for litter-to-litter variation in animal models. BMC Neurosci. 14, 37.
Li, X., Yang, Z., Zhang, A., 2009b. The effect of neurotrophin-3/chitosan carriers on the proliferation and differentiation of neural stem cells. Biomaterials 30 (28), 4978–4985.
Li, X., Yang, Z., Zhang, A., Wang, T., Chen, W., 2009a. Repair of thoracic spinal cord injury by chitosan tube implantation in adult rats. Biomaterials 30 (6), 1121–1132.
Luo, Y., Coskun, V., Liang, A., Yu, J., Cheng, L., Ge, W., Shi, Z., Zhang, K., Li, C., Cui, Y., Lin, H., Luo, D., Wang, J., Lin, C., Dai, Z., Zhu, H., Zhang, J., Liu, J., Liu, H., Devellis, J., Horvath, S., Sun, Y.E., Li, S., 2015. Single-cell transcriptome analyses reveal signals to activate dormant neural stem cells. Cell 161 (5), 1175–1186.
Luo, D., Ge, W., Hu, X., Li, C., Lee, C.M., Zhou, L., Wu, Z., Yu, J., Lin, S., Yu, J., Xu, W., Chen, L., Zhang, C., Jiang, K., Zhu, X., Li, H., Gao, X., Geng, Y., Jing, B., Wang, Z., Zheng, C., Zhu, R., Yan, Q., Lin, Q., Ye, K., Sun, Y.E., Cheng, L., 2018. Unbiased transcriptomic analyses reveal distinct effects of immune deficiency in CNS function with and without injury. Protein Cell. https://doi.org/10.1007/s13238-018-0559-y.
Mullen, R.J., Buck, C.R., Smith, A.M., 1992. NeuN, a neuronal specific nuclear protein in vertebrates. Development 116 (1), 201–211.
Prinz, F., Schlange, T., Asadullah, K., 2011. Believe it or not: how much can we rely on published data on potential drug targets? Nat. Rev. Drug Discov. 10 (9), 712.
Steward, O., Popovich, P.G., Dietrich, W.D., Kleitman, N., 2012. Replication and reproducibility in spinal cord injury research. Exp. Neurol. 233 (2), 597–605.
Thomas, L.B., Gates, M.A., Steindler, D.A., 1996. Young neurons from the adult subependymal zone proliferate and migrate along an astrocyte, extracellular matrix-rich pathway. Glia 17 (1), 1–14.
Weller, M.G., 2018. Ten basic rules of antibody validation. Anal Chem Insights 13 (1177390118757462).
Williams, R.R., Henao, M., Pearse, D.D., Bunge, M.B., 2015. Permissive Schwann cell graft/spinal cord interfaces for axon regeneration. Cell Transplant. 24 (1), 115–131.
Yamamoto, S., Yamamoto, N., Kitamura, T., Nakamura, K., Nakafuku, M., 2001. Proliferation of parenchymal neural progenitors in response to injury in the adult rat spinal cord. Exp. Neurol. 172 (1), 115–127.
Yang, Z., Duan, H., Mo, L., Qiao, H., Li, X., 2010. The effect of the dosage of NT-3/chitosan carriers on the proliferation and differentiation of neural stem cells. Biomaterials 31 (18), 4846–4854.
Yang, Z., Zhang, A., Duan, H., Zhang, S., Hao, P., Ye, K., Sun, Y.E., Li, X., 2015. NT3-chitosan elicits robust endogenous neurogenesis to enable functional recovery after spinal cord injury. Proc. Natl. Acad. Sci. U. S. A. 112 (43), 13354–13359.